

# Constraint-based, Single-point Approximate Kinetic Energy Functionals

V.V. Karasiev,<sup>1,2,\*</sup> R. S. Jones,<sup>3</sup> S.B. Trickey,<sup>2,†</sup> and Frank E. Harris<sup>4,2</sup>

<sup>1</sup>*Centro de Química, Instituto Venezolano de Investigaciones Científicas, Apartado 21827, Caracas 1020-A, Venezuela*

<sup>2</sup>*Quantum Theory Project, Departments of Physics and of Chemistry, University of Florida, Gainesville, FL 32611*

<sup>3</sup>*Department of Physics, Loyola College in Maryland, 4501 N. Charles Street, Baltimore, MD 21210*

<sup>4</sup>*Department of Physics, University of Utah, Salt Lake City, UT*

(Dated: 03 September 2008, Version E2b)

We present a substantial extension of our constraint-based approach for development of orbital-free (OF) kinetic-energy (KE) density functionals intended for the calculation of quantum-mechanical forces in multi-scale molecular dynamics simulations. Suitability for realistic system simulations requires that the OF-KE functional yield accurate forces on the nuclei yet be relatively simple. We therefore require that the functionals be based on DFT constraints, local, dependent upon a small number of parameters fitted to a training set of limited size, and applicable beyond the scope of the training set. Our previous “modified conjoint” generalized-gradient-type functionals were constrained to producing a positive-definite Pauli potential. Though distinctly better than several published GGA-type functionals in that they gave semi-quantitative agreement with Born-Oppenheimer forces from full Kohn-Sham results, those modified conjoint functionals suffer from unphysical singularities at the nuclei. Here we show how to remove such singularities by introducing higher-order density derivatives. We give a simple illustration of such a functional used for the dissociation energy as a function of bond length for selected molecules.

PACS numbers: 71.15.Mb, 31.15.xv, 31.15.E-

## I. INTRODUCTION

Simulation of the structure and properties of complicated materials is a demanding task, particularly away from equilibrium, for example, in the simultaneous presence of solvents and mechanical stress. Though the present results are not limited to it, our motivating problem has been tensile fracture of silica in the presence of water.

For such problems, quantum mechanical treatment of the reactive zone is essential at least at the level of realistic Born-Oppenheimer (B-O) forces to drive an otherwise classical molecular dynamics (MD) or molecular mechanics (MM) calculation. Computational cost then leads to a nested-region strategy. Internuclear forces in the reactive zone are obtained from an explicitly quantum mechanical treatment. Forces between other nuclei are calculated from classical potentials. Such partitioning is called multi-scale simulation in the computational materials community and QM/MD (or QM/MM) methodology in computational molecular biology.

The QM calculation is the computationally rate-limiting step. QM approximations good enough yet computationally fast on the scale of the MD algorithms are therefore critical. Both the inherent form and the growing dominance of density functional theory (DFT) for describing molecular, bio-molecular, and materials systems make it a reasonable candidate QM. Despite advances in pseudopotentials and order- $N$  approximations, however, solution of the DFT Kohn-Sham (KS) problem is too slow computationally to be fully satisfactory. An alternative, Car-Parrinello dynamics<sup>1</sup>, does not guarantee that the motion is restricted to the B-O energy surface.

Thus there is continuing need for methods which

yield essentially full DFT accuracy at significantly lower computational cost. In response, we and co-workers proposed and demonstrated a Graded Sequence of Approximations<sup>2</sup> scheme. Its essence is use of a simple, classical potential for the majority of MD steps, with periodic correction by calibration to forces obtained from more accurate but slower methods. An example Graded Sequence of Approximations would be: (1) classical potential; (2) simple reactive (charge re-distribution) potential<sup>3,4,5</sup>; (3) Orbital-free (OF) DFT, the subject of this paper; (4) Quasi-spin density DFT<sup>6</sup> (a way to approximate spin-dependent effects at the cost of non-spin-polarized KS-DFT); (5) Full spin-polarized DFT (the level of refinement ultimately required for bond-breaking).

In this hierarchy, a large gap in computational cost separates reactive potentials and quasi-spin density DFT. Since the cost of conventional KS calculations comes from solving for the KS orbitals, an obvious candidate to fill the gap is OF-DFT. The long-standing problem is a suitable OF approximation to the kinetic energy (KE). Background about the problem and a detailed description of our first OF-KE functionals were reported in a paper addressed to the computational materials science community<sup>7</sup>, with a more didactic survey in Ref. 8. The present analysis focuses on identifying the causes of limitations of those functionals and ways to eliminate those limitations.

## II. BACKGROUND SUMMARY

Construction of an accurate, explicit total electronic kinetic energy density functional  $T[n] = \langle \Psi | \hat{T} | \Psi \rangle$  for a

many-electron system in state  $|\Psi\rangle$  with electron number density  $n$  is an unresolved task<sup>9,10,11</sup>. The Coulomb virial theorem suggests that the task is equivalent to seeking the total energy functional itself. The Kohn-Sham KE is thus a more attractive target for multiple reasons. Of course, the appeal of OF-DFT predates modern DFT, as witness the Thomas-Fermi-Dirac<sup>12,13</sup> and von Weizsäcker<sup>14</sup> models. There has been considerable activity more recently. A review with extensive references is given in Ref. 15. Other relevant work is that of Carter and co-workers; a helpful review with many references is Ref. 16. More recent developments include, for example, Refs. 17,18,19,20,21,22 as well as our own work already cited.

Distinct from most other recent efforts, our approach is to construct *one-point, i.e., local* approximate KE functionals specifically for MD computations. We insist on constraint-based forms and parameters, that is, satisfaction of known exact results for positivity, scaling, and the like. We are willing, as needed, to simplify the search by requiring only that the functional give adequate interatomic forces, not total energies (and certainly not KS band structures nor general linear response).

To summarize basics and set notation, we first note that except as indicated otherwise we use Hartree atomic units. The Kohn-Sham<sup>23</sup> kinetic energy  $T_s$ , the major contribution to  $T$ , is defined in terms of the KS orbitals:

$$\begin{aligned} T_s[\{\phi_i\}_{i=1}^N] &= \sum_{i=1}^N \int \phi_i^*(\mathbf{r}) \left(-\frac{1}{2}\nabla^2\right) \phi_i(\mathbf{r}) d^3\mathbf{r} \\ &\equiv \int t_{\text{orb}}(\mathbf{r}) d^3\mathbf{r}. \end{aligned} \quad (1)$$

The remainder,  $T - T_s$ , is included in the exchange-correlation (XC) functional  $E_{\text{xc}}[n]$ . Since successful  $E_{\text{xc}}$  approximations assume this KS KE decomposition, we focus on  $T_s$ . This approach also evades the formidable task associated with the full  $T[n]$  just mentioned.

For  $T_s[n]$  an explicit functional of  $n$ , the DFT total energy functional is orbital-free:

$$\begin{aligned} E^{\text{OF-DFT}}[n] &= T_s[n] + E_{\text{Ne}}[n] + E_{\text{H}}[n] \\ &\quad + E_{\text{xc}}[n] + E_{\text{NN}}. \end{aligned} \quad (2)$$

Here  $E_{\text{Ne}}[n]$  is the nuclear-electron interaction energy functional,  $E_{\text{H}}[n]$  is the Hartree functional (classical electron-electron repulsion), and  $E_{\text{NN}}$  is the inter-nuclear repulsion. Then the variational principle gives the single Euler equation

$$\frac{\delta T_s[n]}{\delta n(\mathbf{r})} + v_{\text{KS}}([n]; \mathbf{r}) = \mu, \quad (3)$$

where  $\mu$  is the Lagrange multiplier for density normalization  $\int n(\mathbf{r}) d^3\mathbf{r} = N$  at the nuclear configuration  $\mathbf{R}_1, \mathbf{R}_2, \dots$ , and  $v_{\text{KS}} = \delta(E_{\text{Ne}} + E_{\text{H}} + E_{\text{xc}})/\delta n$ . The force

on nucleus  $I$  at  $\mathbf{R}_I$  is simply

$$\begin{aligned} \mathbf{F}_I &= -\nabla_{\mathbf{R}_I} E^{\text{OF-DFT}} \\ &= -\nabla_{\mathbf{R}_I} E_{\text{NN}} - \int n(\mathbf{r}) \nabla_{\mathbf{R}_I} v_{\text{Ne}} d^3\mathbf{r} \\ &\quad - \int \left[ \frac{\delta T_s[n]}{\delta n(\mathbf{r})} + v_{\text{KS}}([n]; \mathbf{r}) \right] \nabla_{\mathbf{R}_I} n(\mathbf{r}) d^3\mathbf{r}. \end{aligned} \quad (4)$$

The third term in Eq. (4) shows that the biggest error in the calculated force will come from the gradient of the approximate  $T_s[n]$  functional, because the kinetic energy is an order of magnitude larger than the magnitude of  $E_{\text{xc}}$  (which also must be approximated in practice). As will be discussed, when the development of approximate KE functionals focuses on forces, it is convenient to use Eq. (4) with number density  $n(\mathbf{r})$  from a conventional KS calculation (with a specific approximate  $E_{\text{xc}}$ ) as input.

In constructing approximate functionals it is quite common to begin with the Thomas-Fermi functional<sup>12,13</sup>,

$$\begin{aligned} T_{\text{TF}}[n] &= c_0 \int n^{5/3}(\mathbf{r}) d^3\mathbf{r} \equiv \int t_0(\mathbf{r}) d^3\mathbf{r}, \\ c_0 &= \frac{3}{10} (3\pi^2)^{2/3}. \end{aligned} \quad (5)$$

By itself, the TF functional is not an acceptable approximation, because of, for example, the Teller non-binding theorem<sup>24</sup>. A more productive route for our purposes is to decompose  $T_s[n]$  into the von Weizsäcker energy  $T_{\text{W}}^{14}$ , plus a *non-negative* remainder, known as the Pauli term  $T_{\theta}^{25,26,27,28}$ ,

$$T_s[n] = T_{\text{W}}[n] + T_{\theta}[n], \quad T_{\theta}[n] \geq 0 \quad (6)$$

with

$$T_{\text{W}}[n] = \frac{1}{8} \int \frac{|\nabla n(\mathbf{r})|^2}{n(\mathbf{r})} d^3\mathbf{r} \equiv \int t_{\text{W}}[n(\mathbf{r})] d^3\mathbf{r}. \quad (7)$$

Previously we have shown<sup>7</sup> that the non-negativity of  $T_{\theta}$  and  $t_{\theta}(\mathbf{r})$ , defined by

$$\begin{aligned} T_{\theta} &= \int t_{\theta}(\mathbf{r}) d^3\mathbf{r} \\ t_{\theta} &\equiv t_{\text{orb}} - \sqrt{n} \frac{1}{2} \nabla^2 \sqrt{n} \end{aligned} \quad (8)$$

is a crucial but not sufficient condition for determining a realistic OF-KE approximation. Details of some remaining issues follow.

### III. GGA-TYPE KE FUNCTIONALS AND THEIR LIMITATIONS

#### A. Basic structure

Pursuit of local approximations for  $t_{\text{orb}}(\mathbf{r}) = t_{\text{W}}[n(\mathbf{r}), \nabla n(\mathbf{r})] + t_{\theta}[n(\mathbf{r}), \nabla n(\mathbf{r}), \dots]$  stimulates consid-

eration of a counterpart to the generalized gradient approximation (GGA) for XC<sup>29</sup>, namely

$$T_s^{\text{GGA}}[n] = c_0 \int n^{5/3}(\mathbf{r}) F_t(s(\mathbf{r})) d^3\mathbf{r}. \quad (9)$$

Here  $s$  is a dimensionless reduced density gradient

$$s \equiv \frac{|\nabla n|}{2nk_F}, \quad k_F \equiv (3\pi^2 n)^{1/3}. \quad (10)$$

$F_t$  is a kinetic energy enhancement factor which goes to unity for uniform density. Equation (9) is motivated in part by the conjointness conjecture<sup>30</sup>, which posits that  $F_t(s) \propto F_x(s)$  where  $F_x$  is the enhancement factor in GGA exchange. We showed previously that this relationship cannot hold strictly<sup>7</sup>, but the form is suggestive and useful.

For connection with  $T_\theta \geq 0$ , we re-express  $T_W$  in a form parallel with Eq. (9). From Eqs. (7) and (10),

$$T_W[n] = c_0 \int n^{5/3}(\mathbf{r}) \frac{5}{3} s^2(\mathbf{r}) d^3\mathbf{r}. \quad (11)$$

Then Eq. (6) gives

$$T_s^{\text{GGA}}[n] = T_W[n] + c_0 \int n^{5/3}(\mathbf{r}) F_\theta(s(\mathbf{r})) d^3\mathbf{r}, \quad (12)$$

where

$$F_\theta(s) = F_t(s) - \frac{5}{3} s^2. \quad (13)$$

The final term of Eq. (12) thus is a formal representation of the GGA Pauli term  $T_\theta^{\text{GGA}}$ . Note that the form of Eq. (12) automatically preserves proper uniform scaling of  $T_s$  (see Ref. 31):

$$\begin{aligned} T_s[n_\gamma] &= \gamma^2 T_s[n], \\ n_\gamma(\mathbf{r}) &\equiv \gamma^3 n(\gamma\mathbf{r}). \end{aligned} \quad (14)$$

Constraints that must be satisfied by the enhancement factors associated with any satisfactory GGA KE functional include

$$t_\theta([n]; \mathbf{r}) \geq 0, \quad (15)$$

as well as<sup>28,32,33</sup>

$$v_\theta([n]; \mathbf{r}) = \delta T_\theta[n] / \delta n(\mathbf{r}) \geq 0, \quad \forall \mathbf{r}. \quad (16)$$

The quantity  $v_\theta$  is known as the Pauli potential. Constraint Eq. (15) implies the non-negativity of the GGA enhancement factor,  $F_\theta(s(\mathbf{r})) \geq 0$ .

For a slowly varying density that is not itself small, we have  $s \approx 0$ , and it is appropriate to write  $T_s$  as a gradient expansion<sup>34</sup>:

$$T_s[n] = T_{\text{TF}}[n] + \frac{1}{9} T_W[n] + \text{higher order terms}. \quad (17)$$

Truncation at second order in  $s$  gives the second-order gradient approximation (SGA), with the SGA enhancement factor<sup>29</sup>

$$F_t^{\text{SGA}}(s) = 1 + \frac{1}{9} \cdot \frac{5}{3} s^2 = 1 + \frac{5}{27} s^2, \quad (18)$$

or

$$F_\theta^{\text{SGA}}(s) = 1 - \frac{40}{27} s^2. \quad (19)$$

These forms should be exhibited by the exact functional in the limit of small density variation. (Though there are  $s \rightarrow \infty$  constraints<sup>11</sup>, we have not used them so far.)

For GGA functionals,  $v_\theta$ , Eq. (16), can be written<sup>35,36</sup> as

$$\frac{\delta T_\theta^{\text{GGA}}}{\delta n(\mathbf{r})} = \frac{\partial t_\theta[n(\mathbf{r}), \nabla n(\mathbf{r})]}{\partial n(\mathbf{r})} - \nabla \cdot \frac{\partial t_\theta[n(\mathbf{r}), \nabla n(\mathbf{r})]}{\partial (\nabla n(\mathbf{r}))}. \quad (20)$$

After some tedium, one finds

$$\begin{aligned} v_\theta^{\text{GGA}} &= \frac{5}{3} c_0 n^{2/3} F_\theta + \\ & c_0 n^{5/3} \frac{\partial F_\theta}{\partial s} \left[ \frac{\partial s}{\partial n} - \frac{5}{3} \frac{\nabla n}{n} \cdot \frac{\partial s}{\partial \nabla n} - \nabla \cdot \frac{\partial s}{\partial \nabla n} \right] \\ & - c_0 n^{5/3} \frac{\partial^2 F_\theta}{\partial s^2} \left( \nabla s \cdot \frac{\partial s}{\partial \nabla n} \right). \end{aligned} \quad (21)$$

(The last line was omitted in Eq. (34) of Ref. 7 but included in the actual numerical work.) A somewhat cleaner expression that also makes it easier to understand the extension we present below comes from shifting to the variable  $s^2$  and defining both the reduced Laplacian density  $p$

$$p \equiv \frac{\nabla^2 n}{(2k_F)^2 n} = \frac{\nabla^2 n}{4(3\pi^2)^{2/3} n^{5/3}}, \quad (22)$$

and one of the various possible dimensionless fourth-order derivatives  $q$

$$q \equiv \frac{\nabla n \cdot (\nabla \nabla n) \cdot \nabla n}{(2k_F)^4 n^3} = \frac{\nabla n \cdot (\nabla \nabla n) \cdot \nabla n}{16(3\pi^2)^4 / 3 n^{13/3}} \quad (23)$$

(Note that our  $s^2$ ,  $p$  are denoted as  $p$ ,  $q$  respectively in Ref. 19.) Then Eq. (21) becomes

$$\begin{aligned} v_\theta^{\text{GGA}}(s^2) &= c_0 n^{2/3} \left\{ \frac{5}{3} F_\theta(s^2) - \left( \frac{2}{3} s^2 + 2p \right) \frac{\partial F_\theta}{\partial (s^2)} \right. \\ & \left. + \left( \frac{16}{3} s^4 - 4q \right) \frac{\partial^2 F_\theta}{\partial (s^2)^2} \right\}. \end{aligned} \quad (24)$$

See Appendix A for details.

## B. Singularities

Near a point nucleus of charge  $Z$  at the origin, the number density behaves to first order in  $r$  as

$$n(\mathbf{r}) \sim (1 - 2Z|\mathbf{r}|) + O(|\mathbf{r}|^2) \quad (25)$$

as required by Kato’s cusp condition<sup>37,38,39,40,41</sup>. Sufficiently close to a nucleus therefore,  $n(\mathbf{r})$  behaves as a Hydrogen-like 1s-electron density

$$n_H(\mathbf{r}) \sim \exp(-2Z|\mathbf{r}|) \quad (26)$$

That is, the variation of  $n'(r)/n(r)$  is equal for these densities sufficiently close to the nucleus, hence the form in Eq. (26) is a reasonable near-nucleus approximation<sup>42</sup>. Consequences of differences in the higher-order terms in the respective Taylor expansions of actual and hydrogenic 1s densities are discussed in Section IV-A. Also see Ref. 43 for a related discussion.

For  $n(\mathbf{r})$  of the form of Eq. (26) near  $r = 0$ ,  $s$  and  $q$  remain finite while  $p \rightarrow -4Z/(2k_F)^2 r$ . In this case, Eq. (24) becomes

$$v_\theta^{\text{GGA}}(r \rightarrow 0) = \frac{3Z}{5r} \frac{\partial F_\theta^{\text{GGA}}}{\partial(s^2)} + \text{nonsingular terms.} \quad (27)$$

If  $s^2$  is sufficiently small that it is a good approximation to write  $F_\theta^{\text{GGA}} \approx 1 + as^2$  (note that this is exactly the form of  $F_\theta^{\text{SGA}}$ ), Eq. (27) simplifies to

$$v_\theta^{\text{GGA}}(r \rightarrow 0) = \frac{3aZ}{5r} + \text{nonsingular terms,} \quad (28)$$

in which case  $v_\theta^{\text{GGA}}$  tends to infinity at the nuclei with the same sign as the GGA parameter  $a$ . The small values of  $s^2$  at the nuclei make this a general phenomenon. (Near typical nuclei ( $r \rightarrow 0$ ), numerical experience shows that  $s^2 \approx 0.15$ , so that the small- $s^2$  behavior of any  $F_\theta(s^2)$  of GGA form is relevant there.)

Equation (28) shows that purely GGA Pauli potentials have singularities in the vicinity of nuclear sites. In contrast, calculations using KS quantities as inputs show that the exact Pauli potential is finite at the nuclei (see, for example, Ref. 26 as well as Fig. 2 below). Moreover, the positivity requirement for  $v_\theta$  will certainly be violated near the nuclei both for  $F_\theta^{\text{SGA}}$  and for any GGA form with  $a < 0$ .

### C. Positivity: tests and enforcement

To explore these positivity constraints, we tested six published KE functionals<sup>44,45,46,47,48,49</sup> that either are strictly conjoint or are based closely on conjointness. The test used the diatomic molecule SiO, an important reference species for us. With LDA XC, we did a conventional, orbital-dependent, KS calculation as a function of bond length (details are in Appendix B). At each bond length, the converged KS density was used as input to the orbital-free  $E[n]$  corresponding to one of the six  $T_s[n]$  approximations. None predicted a stable SiO molecule. All six produced  $a \leq 0$  in Eq. (28), hence all six have non-trivial violations of  $v_\theta$  positivity, with all the effective enhancement factors very close to that of the SGA,  $F_\theta(s) = 1 - 40/27s^2$ . Details are in Refs. 7 and 8. Because of the constraint violation, conjointness thus can, at most, be a guide.

We enforced positivity of  $v_\theta^{\text{GGA}}$  by particular parameterization of  $F_t(s)$  forms based, in part, on the Perdew, Burke, and Ernzerhof (PBE)<sup>45</sup> GGA XC form:

$$F_t^{\text{PBE}\nu}(s) = 1 + \sum_{i=1}^{\nu-1} C_i \left[ \frac{s^2}{1 + a_1 s^2} \right]^i, \quad \nu = 2, 3, 4$$

$$F_t^{\text{exp4}}(s) = C_1(1 - e^{-a_1 s^2}) + C_2(1 - e^{-a_2 s^4}). \quad (29)$$

Our PBE2 form is the same as that used (with different parameters) by Tran and Wesolowski<sup>44</sup> while PBE3 corresponds to the form introduced by Adamo and Barone<sup>46</sup>, but, again, with different parameters. Quite similar forms also were explored by King and Handy<sup>50</sup> in the context of directly fitting a KS kinetic potential  $v_s = \delta T_s / \delta n$  to conventional KS eigenvalues and orbitals; see Eq. (33) below.

We fitted the parameters in the enhancement factors, Eqs. (29), to match the conventional KS inter-nuclear forces for various nuclear configurations of a three-molecule training set: SiO, H<sub>4</sub>SiO<sub>4</sub>, and H<sub>6</sub>Si<sub>2</sub>O<sub>7</sub>. With conventional KS densities as input, we found semi-quantitative agreement with the conventional KS calculations for single bond stretching in H<sub>4</sub>SiO<sub>4</sub>, H<sub>6</sub>Si<sub>2</sub>O<sub>7</sub>, H<sub>2</sub>O, CO, and N<sub>2</sub>. All had energy minima within 5 to 20% of the conventional KS equilibrium bond-length values. The latter two molecules provide particular encouragement, since no data on C or N was included in the parameterization. Details, including parameter values, are in Ref. 7.

### D. Analysis of fitted functional behavior

Despite this progress, there is a problem. Although the PBE $\nu$  and exp4 forms can give Pauli potentials that are everywhere positive, yielding  $a > 0$  in Eq. (28), they are singular at the nuclei, in contrast to the negative singularities of previously published forms. For clarity about the developments which follow, observe that these nuclear-site singularities occur in  $v_\theta$ , hence are distinct from the intrinsic nuclear-site singularity of the von Weizsäcker potential, which by operation on Eq. (7) can be shown to be

$$v_W \equiv \frac{\delta T_W[n]}{\delta n(\mathbf{r})} = \frac{1}{8} \left[ \frac{|\nabla n|^2}{n^2} - \frac{2 \nabla^2 n}{n} \right]. \quad (30)$$

The intrinsic singularity near a nucleus follows from Eq. (25) and has the form

$$v_W = -\frac{2Z}{r}. \quad (31)$$

Insight regarding the behavior of our modified conjoint functionals can be gained from consideration of the energy density  $dT_\theta^{\text{appx}}(s)/ds$  as a function of  $s$  for various functionals indicated by the generic superscript “appx”. This quantity comes from differentiation of the integrated

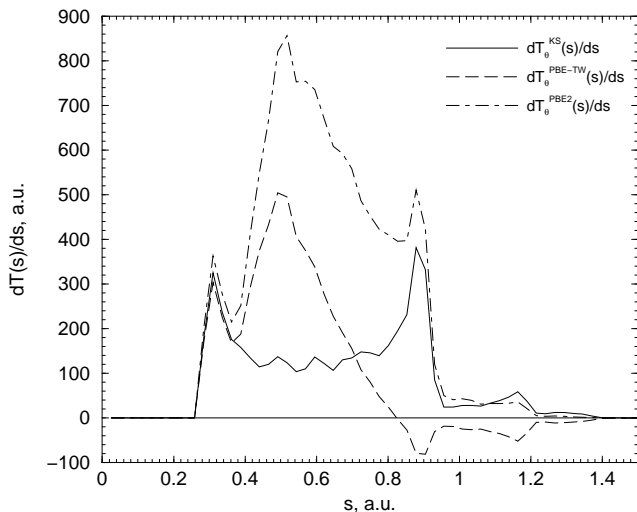


FIG. 1: Energy density contributions to the Pauli term  $T_\theta$  as a function of  $s$ , presented as values of  $dT_\theta(s)/ds$  from Eq. (32); shown are conventional Kohn-Sham  $dT_\theta^{\text{KS}}(s)/ds$  (the reference), our PBE2 functional, and the older PBE-TW GGA functional. Data are for the SiO diatomic molecule at bond length 1.926 Å and are based on the density from fully numerical KS-LDA computations.

contribution  $T_\theta^{\text{appx}}(s)$  of the region  $s(\mathbf{r}) \leq s$  to the kinetic energy:

$$\begin{aligned} T_\theta^{\text{appx}}(s) &\equiv \int_{s(\mathbf{r}) \leq s} t_\theta^{\text{appx}}([n]; \mathbf{r}) d^3\mathbf{r} \\ &= \int_0^s ds \int t_\theta^{\text{appx}}([n]; \mathbf{r}) \delta(s - s(\mathbf{r})) d^3\mathbf{r}. \end{aligned} \quad (32)$$

Figure 1 shows  $dT_\theta^{\text{appx}}(s)/ds$  for the SiO molecule at bond length  $R = 1.926$  Å (slightly stretched). Values are shown for our recent parameterization PBE2 that respects positivity, the Tran-Wesolowski parameterization of the same form (PBE-TW), and for the exact, orbital-dependent KS Pauli term calculated from<sup>28</sup>

$$t_\theta^{\text{KS}} = t_{\text{orb}} - \left( \frac{1}{8} \frac{|\nabla n|^2}{n} - \frac{1}{4} \nabla^2 n \right), \quad (33)$$

where  $t_\theta$  and  $t_{\text{orb}}$  are defined in Eqs. (8) and (1) respectively. Recall that the exact value of  $t_\theta$  must be non-negative<sup>28</sup>. For clarity, note also that while  $t_{\text{orb}}$  can be negative, the equivalent form

$$t_s \equiv t_{\text{orb}} + \frac{1}{4} \nabla^2 n \quad (34)$$

is positive definite<sup>11</sup>.

Figure 1 also shows that both approximate functionals closely resemble the exact KS kernel for  $0.24 < s < 0.38$ . But both of them have a much larger second peak around  $s \approx 0.5$ . In contrast, the exact functional actually has a long low region before a second peak at  $s \approx 0.9$ . Our PBE2 approximate functional mimics the true second

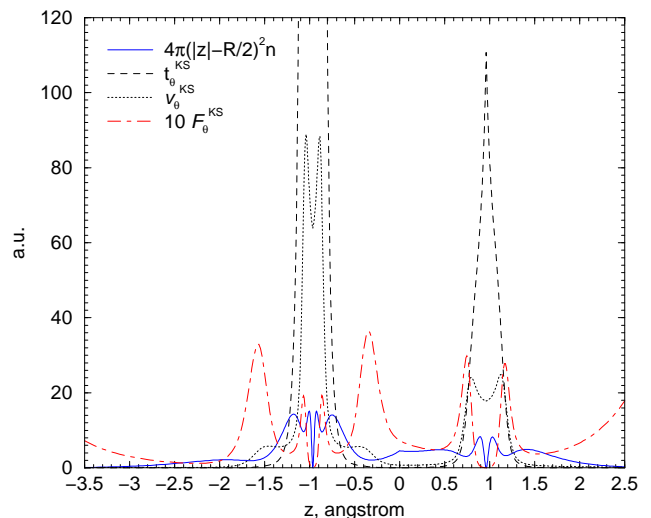


FIG. 2: Conventional (reference) KS values for electronic density (scaled by the factor  $4\pi(|z| - R/2)^2$ , with  $R$  the internuclear distance), Pauli term  $t_\theta$ , Pauli potential  $v_\theta$ , and enhancement factor  $F_\theta$ , calculated for points on the internuclear axis using KS LDA fully numerical orbitals for the SiO molecule; Si at  $(0, 0, -0.963)$ Å, O at  $(0, 0, +0.963)$ Å.

peak via a too-strong third peak while the conventional GGA PBE-TW functional has a spurious minimum at this point. Moreover, the PBE-TW Pauli term goes negative for all  $s > 0.82$ . In addition, we see from Fig. 1 that the KS kinetic energy is nearly totally determined by the behavior of  $F_\theta$  over a relatively small range of  $s$ , approximately  $0.26 \leq s \leq 1.30$  for the SiO diatomic. The asymptotic regions ( $s \rightarrow 0$  and  $s \rightarrow \infty$ ) do not play a significant role. The range  $0.26 \leq s \leq 0.9$  has the highest weight of contribution (the highest differential contribution). As an aside, we remark that PBE2 overestimates the KE presumably because it was fitted purely to forces without regard to total energies.

Figures 2, 3, and 4 provide comparisons of the reference  $t_\theta^{\text{KS}}$ ,  $v_\theta^{\text{KS}}$ , and  $F_\theta^{\text{KS}}$  (where  $F_\theta^{\text{KS}} \equiv t_\theta^{\text{KS}}/c_0 n^{5/3}$ ) with the corresponding quantities for the PBE-TW and PBE2 approximations. The values are along the internuclear axis of the SiO molecule with internuclear separation 1.926 Å. The KS Pauli potential was calculated using the exact orbital-dependent expression

$$v_\theta([n]; \mathbf{r}) = \frac{t_\theta([n]; \mathbf{r})}{n(\mathbf{r})} + \sum_{i=1}^N (\varepsilon_N - \varepsilon_i) \frac{|\phi_i(\mathbf{r})|^2}{n(\mathbf{r})}, \quad (35)$$

where  $\phi_i$  and  $\varepsilon_i$  are the occupied KS orbitals and eigenvalues respectively. Equation (35) is obtained in a way similar to that used in Ref. 28; see Ref. 8.

In Fig. 2, all three KS quantities,  $t_\theta^{\text{KS}}$ ,  $v_\theta^{\text{KS}}$ , and  $F_\theta^{\text{KS}}$  are everywhere *non-negative*, as they must be. Observe that  $v_\theta^{\text{KS}}$  is *finite* at the nuclei and has local maxima in positions close to the inter-shell minima of the electronic density.

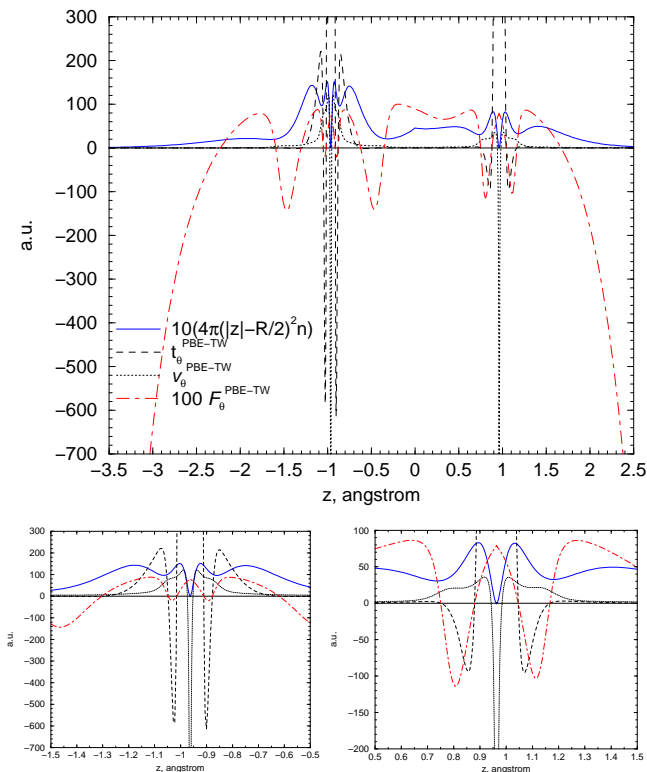


FIG. 3: As in Fig. 2 for the PBE-TW conjoint approximation. Lower left panel: region near Si-center; Lower right panel: region near O-center.

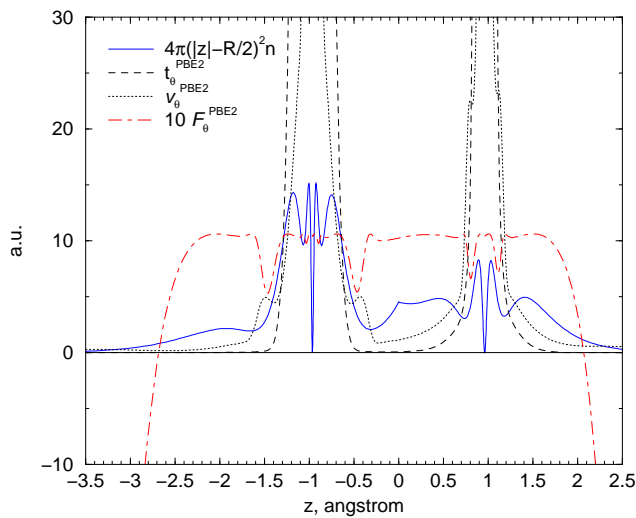


FIG. 4: As in Fig. 2 for the PBE2 modified-conjoint approximation.

In contrast, the energy density of the PBE-TW Pauli term and corresponding enhancement factor have negative peaks in the inter-shell regions, violations of the non-negativity constraint for  $t_\theta$ . However, addition to  $t_\theta^{\text{appx}}$  of any multiple of a Laplacian term  $\nabla^2 n$  would change only the local behavior without altering the value of  $T_\theta^{\text{appx}}[n]$ ,

so the PBE-TW misbehavior might be resolved by such an addition. See discussion below. Figure 3 also shows that  $v_\theta$  for the PBE-TW functional has very sharp negative peaks exactly at the nuclear positions, in accord with Eq. (28).

Figure 4 shows that the modified conjoint PBE2  $v_\theta$  respects the positivity constraint everywhere. Inter-nuclear forces in the attractive region are described at least qualitatively correctly as a result. The PBE2 potential is still divergent at the nuclei in accordance with Eq. (28).

As an aside we remark on two small computational issues. First, the absence of nuclear-site singularities in the computed correct Pauli potentials  $v_\theta^{\text{KS}}$  might be argued to occur because the computed density does not have precisely the proper nuclear site cusp, i.e., does not strictly obey Eq. (25). However, our numerical results are consistent with those in Ref. 26. Those authors used numerical orbitals<sup>51</sup> which presumably satisfied the cusp condition approximately. More importantly, if a specific numerical technique gives a KS density and associated KS  $t_s$  that produce a non-singular  $v_\theta$ , then an approximate  $v_\theta$  evaluated with the *same* density should not introduce singularities. Second, the reader may notice that Fig. 4 shows small negative values for  $t_\theta$  far from the bonding region of the molecule. This behavior is due to numerical imprecision associated with computation for extremely small values of the density, and makes no appreciable contribution to the kinetic energy.

Finally, an insight to the harm of excess positivity of  $v_\theta$  can be seen by examining the dependence of  $T_\theta[n]$  upon  $v_\theta$ . From a known virial relation<sup>28</sup> we have

$$T_\theta[n] = \frac{1}{2} \int v_\theta([n]; \mathbf{r})(3 + \mathbf{r} \cdot \nabla)n(\mathbf{r})d^3\mathbf{r}. \quad (36)$$

Any spurious singularities of  $v_\theta^{\text{appx}}$  at the nuclei clearly will cause special problems in overweighting the integrand.

#### IV. BEYOND GGA-TYPE FUNCTIONALS

The preceding analysis makes clear the need for more flexible functionals than the forms of Eq. (29). In particular, nuclear site divergences of  $v_\theta$  are unavoidable for all purely GGA-type functionals *e.g.*, GGA, GGA-conjoint, and modified conjoint KE functionals; recall Eqs. (27) and (28). Additional variables and constraints upon them are required to eliminate the singularities.

##### A. Reduced derivatives of the density

Consider again the gradient expansion of  $T_s[n]$ , Eq. (17) (see Refs. 34, 52,53,54 for details), which we recast as

$$T_s[n] = \int \left\{ t_0([n]; \mathbf{r}) + t_2([n]; \mathbf{r}) + t_4([n]; \mathbf{r}) + \dots \right\} d^3\mathbf{r}. \quad (37)$$

Here  $t_0$  is as in Eq. (5),  $t_2 = (1/9)t_W$ , and

$$t_4([n]; \mathbf{r}) = \frac{1}{540(3\pi^2)^{2/3}} n^{5/3}(\mathbf{r}) \left[ \left( \frac{\nabla^2 n(\mathbf{r})}{n^{5/3}(\mathbf{r})} \right)^2 - \frac{9}{8} \left( \frac{\nabla n(\mathbf{r})}{n^{4/3}(\mathbf{r})} \right)^2 \left( \frac{\nabla^2 n(\mathbf{r})}{n^{5/3}(\mathbf{r})} \right) + \frac{1}{3} \left( \frac{\nabla n(\mathbf{r})}{n^{4/3}(\mathbf{r})} \right)^4 \right] \quad (38)$$

The sixth-order term, dependent upon  $n$ ,  $|\nabla n|$ ,  $\nabla^2 n$ ,  $|\nabla \nabla^2 n|$ , and  $\nabla^4 n$ , is given in Ref. 52.

As is well-known, in a finite system (e.g. molecule), a Laplacian-dependent term  $\nabla^2 n$  affects only the local behavior of the kinetic energy density. Arguments have been advanced for and against including such Laplacian dependence in the KE density functional; for example, see Refs. 50, 54, 55. Recently Perdew and Constantin<sup>19</sup> presented a KE functional that depends on  $\nabla^2 n$  via a modified fourth-order gradient expansion. Though not stated that way, their functional obeys the decomposition of Eq. (6). It is intended to be universal (or at least very broadly applicable), whereas we are focused on simpler functionals that require parameterization to families of systems. The Perdew-Constantin form involves a rather complicated functional interpolation between the gradient expansion and the von Weizsäcker functional. They did not discuss the corresponding potential  $v_\theta$  nor Born-Oppenheimer forces. And they characterized the performance of their functional for the energetics of small molecule dissociation as “still not accurate enough for chemical applications”. So we proceed rather differently.

Rearrange the foregoing gradient expansion into  $T_W + T_\theta$  form (recall Eq. (6)):

$$\begin{aligned} T_\theta[n] &= \int \left[ c_0 n^{5/3}(\mathbf{r}) \left( 1 - \frac{40}{27} s^2 \right) + t_4 + t_6 + \dots \right] d^3 \mathbf{r} \\ &= \int \left[ t_0 \left( 1 - \frac{5}{3} s^2 \right) + t_0 \frac{5}{27} s^2 + t_4 + t_6 + \dots \right] d^3 \mathbf{r} \\ &\equiv \int \left[ t_\theta^{(0)}([n]; \mathbf{r}) + t_\theta^{(2)}([n]; \mathbf{r}) + t_\theta^{(4)}([n]; \mathbf{r}) + \dots \right] d^3 \mathbf{r} \end{aligned} \quad (39)$$

where

$$t_\theta^{(0)}([n]; \mathbf{r}) = t_0([n]; \mathbf{r}) \left[ 1 - \frac{5}{3} s^2 \right], \quad (40)$$

$$t_\theta^{(2)}([n]; \mathbf{r}) = t_0([n]; \mathbf{r}) \left[ \frac{5}{27} s^2 \right], \quad (41)$$

and

$$t_\theta^{(4)}([n]; \mathbf{r}) = t_0([n]; \mathbf{r}) \left[ \frac{8}{81} \left( p^2 - \frac{9}{8} s^2 p + \frac{1}{3} s^4 \right) \right]. \quad (42)$$

Each term, Eq. (40)–(42), of Eq. (39) can be put straightforwardly into a GGA-like form:

$$t_\theta^{(2i)}([n]; \mathbf{r}) = t_0([n]; \mathbf{r}) F_\theta^{(2i)}(s, p, \dots), \quad (43)$$

where  $s$ ,  $p$  are as in Eqs. (10) and (22) respectively. The first two terms of the expansion yield the SGA enhancement factor already discussed

$$F_\theta^{\text{SGA}} \equiv F_\theta^{(0)} + F_\theta^{(2)} = 1 + a_2 s^2, \quad (44)$$

with  $a_2 = -40/27$ . The fourth-order (in highest power of  $s$ ) term is

$$F_\theta^{(4)} = a_4 s^4 + b_2 p^2 + c_{21} s^2 p, \quad (45)$$

with coefficients  $a_4 = 8/243$ ,  $b_2 = 8/81$ , and  $c_{21} = -1/9$ .

Rather than retain those values of  $a_2$ ,  $a_4$ ,  $b_2$ ,  $c_{21}$ , we instead treat them as parameters and seek values or relationships among them which would yield a non-singular  $v_\theta$  through a given order. (Corresponding improvement of Thomas-Fermi theory by imposition of the nuclear cusp condition was introduced in Ref. 56.)

Functional differentiation of each term in Eq. (39) gives the formal gradient expansion  $v_\theta = v_\theta^{(0)} + v_\theta^{(2)} + v_\theta^{(4)} + \dots$ , where  $F_\theta^{(2i)}$  (shown below with its arguments suppressed for clarity) is a function of  $s^2$ ,  $p$ , and in principle, higher derivatives of  $n(\mathbf{r})$ :

$$\begin{aligned} v_\theta^{(2i)}(\mathbf{r}) &= t_0([n]; \mathbf{r}) \left[ \frac{5}{3n(\mathbf{r})} F_\theta^{(2i)} + \frac{\partial F_\theta^{(2i)}}{\partial (s^2)} \frac{\partial (s^2)}{\partial n(\mathbf{r})} \right. \\ &\quad \left. + \frac{\partial F_\theta^{(2i)}}{\partial p} \frac{\partial p}{\partial n(\mathbf{r})} + \dots \right] \\ &\quad - \nabla \cdot \left( t_0([n]; \mathbf{r}) \frac{\partial F_\theta^{(2i)}}{\partial (s^2)} \frac{\partial (s^2)}{\partial \nabla n(\mathbf{r})} \right) \\ &\quad + \nabla^2 \left( t_0([n]; \mathbf{r}) \frac{\partial F_\theta^{(2i)}}{\partial p} \frac{\partial p}{\partial \nabla^2 n(\mathbf{r})} \right) + \dots \end{aligned} \quad (46)$$

The ellipses in Eq. (46) correspond to additional terms that are needed only if  $F_\theta^{(2i)}$  depends upon derivatives other than  $s$  and  $p$ .

After manipulation (see Appendix A), one obtains the potentials corresponding to the enhancement factors in Eqs. (44) and (45):

$$v_\theta^{\text{SGA}} = c_0 n^{2/3} \left[ \frac{5}{3} + a_2 s^2 - 2a_2 p \right], \quad (47)$$

$$\begin{aligned} v_\theta^{(4)} &= c_0 n^{2/3} \left[ \left( 11a_4 + \frac{88}{9} c_{21} \right) s^4 \right. \\ &\quad - (5b_2 + 2c_{21}) p^2 - \left( 4a_4 - \frac{80}{9} b_2 \right) s^2 p \\ &\quad - \left( 8a_4 + \frac{32}{3} c_{21} \right) q \\ &\quad \left. - \frac{20}{3} b_2 q' + 2b_2 q'' + 2c_{21} q''' \right]. \end{aligned} \quad (48)$$

Here  $q$  is as in Eq. (23) and  $q'$ ,  $q''$ , and  $q'''$  are other dimensionless fourth-order reduced density derivatives defined as

$$q' \equiv \frac{\nabla n \cdot \nabla \nabla^2 n}{(2k_F)^4 n^2} = \frac{\nabla n \cdot \nabla \nabla^2 n}{16(3\pi^2)^{4/3} n^{10/3}}, \quad (49)$$

$$q'' \equiv \frac{\nabla^4 n}{(2k_F)^4 n} = \frac{\nabla^4 n}{16(3\pi^2)^{4/3} n^{7/3}}, \quad (50)$$

$$q''' \equiv \frac{\nabla \nabla n : \nabla \nabla n}{(2k_F)^4 n^2} = \frac{\nabla \nabla n : \nabla \nabla n}{16(3\pi^2)^{4/3} n^{10/3}}. \quad (51)$$

The operation denoted by the colon in the numerators of  $q'''$  is  $A : B \equiv \sum_{ij} A_{ij} B_{ji}$ .

At Eq. (27) we have already pointed out that an enhancement factor of SGA form, specifically, that of Eq. (44), produces a Pauli potential

$$v_\theta^{\text{SGA}}(r) = v_\theta^{(0)}(r) + v_\theta^{(2)}(r) = \frac{3Za_2}{5r} + \text{nonsingular terms}. \quad (52)$$

This exhibits the  $1/r$  SGA Pauli potential nuclear singularity already discussed; we return to this point in a moment.

For the fourth-order enhancement factor, Eq. (45), we again note that  $s$  and  $q$  are non-singular near the nucleus, while

$$\lim_{r \rightarrow 0} s^2(r) = Z^2/[3\pi^2 n(0)]^{2/3}. \quad (53)$$

With a density of the form of Eq. (26), Eq. (48) thus gives the near-nucleus behavior of the fourth-order potential as

$$\begin{aligned} v_\theta^{(4)}(r) &= \frac{c_0}{16[9\pi^4 n(r)]^{2/3}} \left[ -\frac{16Z^2}{3r^2} (5b_2 + 3c_{21}) \right. \\ &\quad \left. + \frac{32Z^3}{9r} (18a_4 + 17b_2 + 18c_{21}) \right] \\ &\quad + \text{nonsingular terms}. \end{aligned} \quad (54)$$

The singularities in  $1/r^2$  and  $1/r$  can be removed by requiring that the numerators of the first two terms of Eq. (54) both vanish, or equivalently

$$\begin{aligned} c_{21} &= -\frac{5}{3}b_2, \\ a_4 &= \frac{13}{18}b_2. \end{aligned} \quad (55)$$

In the spirit of the GGA, we are led to defining a fourth-order reduced density derivative (RDD) as

$$\kappa_4 = s^4 + \frac{18}{13}p^2 - \frac{30}{13}s^2p. \quad (56)$$

This RDD with Eq. (45) gives an enhancement factor

$$F_\theta^{(4)}(\kappa_4) = a_4 \kappa_4, \quad (57)$$

which yields a Pauli potential with *finite* values at point nuclei. Clearly it is not the only  $\kappa_4$ -dependent enhancement factor with that property. So, we seek  $F_\theta^{(4)}(\kappa_4)$  functional forms which are more general than Eq. (57) and which give a positive-definite, non-singular  $v_\theta$ .

At this point, it is prudent to consider how many terms in the Taylor series expansion of the density Eq. (26) are relevant for the cancellation of singularities in Eq. (54). The answer is four terms:  $n(r) \propto 1 - 2Zr + 2Z^2r^2 - (4/3)Z^3r^3$ . That is, the singularities will reappear for a density of the form of Eq. (25) if the second- and third-order terms differ from those defined by a Hydrogen-like density expansion, e.g., Eq. (26). Thus, the foregoing cancellation fails for a density with power series expansion  $n(r) \propto 1 - 2Zr - (4/3)Z^3r^3 + \dots$ . This fact will limit applications of simple  $\kappa_4$ -based KE functionals to those densities which have precisely Hydrogen-like behavior up to fourth order.

It is necessary, therefore, to consider other candidates for RDD variables which would provide cancellation of singularities for the density Eq. (25) independently of hydrogenic higher-order terms in the Taylor series expansion of the density. The observation that  $\kappa_4 \sim \mathcal{O}(\nabla^4)$  suggests that the effective or operational order of  $\nabla$  in such a candidate variable should be reduced to second order. This in turn suggests a candidate variable, still based on the fourth-order gradient expansion Eq. (42), namely

$$F_\theta^{(4-2)} = \sqrt{a_4 s^4 + b_2 p^2 + c_{21} s^2 p}, \quad (58)$$

(compare Eq. (45)). Now consider a density of the form of Eq. (25) but with arbitrary first- and higher-order near-nucleus expansion coefficients,

$$n(r) \sim (1 + C_1 r + C_2 r^2 + C_3 r^3). \quad (59)$$

Following the same lines as those used to reach Eq. (54), one finds

$$v_\theta^{(4-2)}(r) \sim \frac{c_{21}}{\sqrt{b_2}} \frac{1}{r} + \text{nonsingular terms}. \quad (60)$$

The singular term would be eliminated by the choice  $c_{21} = 0$ . The cancellation is universal in that it does not depend on the density expansion coefficients,  $C_i$  (while the singular term prefactor and non-singular terms do, of course, depend on those expansion coefficients). Hence a candidate RDD variable (denoted as  $\tilde{\kappa}_4$ ) which provides cancellation of singular terms in the Pauli potential could be defined as

$$\tilde{\kappa}_4 = \sqrt{s^4 + b_2 p^2}, \quad b_2 > 0. \quad (61)$$

Note that this form is manifestly positive.

This RDD can be used to construct a variety of enhancement factors to replace Eq. (45) for the fourth-order approximation to the Pauli term, for example  $F_\theta(\tilde{\kappa}_4) = a_4 \tilde{\kappa}_4$ . This simplest enhancement factor corresponds to a Pauli potential with *finite* values at point



nuclei but clearly it is not the only  $\tilde{\kappa}_4$ -dependent one with that property. Any linear combination of non-singular enhancement factors (including the simple  $F_\theta = 1$ ) also will be non-singular. A combination of two PBE-like forms (see Eq. (68) below) is also non-singular, as can be checked analytically for any density with near-nucleus behavior defined by Eq. (59), hence also Eqs. (25), (26).

There are, of course,  $\tilde{\kappa}_4$ -dependent functionals that yield a divergent potential, e.g.

$$F_\theta(\tilde{\kappa}_4) = \tilde{\kappa}_4^2 \quad (62)$$

so one must be cautious.

Regarding the second-order forms, Eq. (52) shows that, short of complete removal of the  $s^2$  term from  $F_\theta^{\text{SGA}}$ , we cannot cure the singularity in  $v_\theta^{\text{SGA}}$ . There is no direct analogy to the removal of singularities in  $v_\theta^{(4)}$  just discussed. Instead, in parallel with Eq. (56) or Eq. (61), we introduce a second-order RDD

$$\kappa_2 = s^2 + b_1 p, \quad (63)$$

with  $b_1$  to be determined. Then, in analogy with a PBE-type enhancement factor, we can define an enhancement factor dependent only on second-order variables as

$$F_\theta^{(2)}(\kappa_2) = \frac{\kappa_2}{1 + \alpha \kappa_2}. \quad (64)$$

For it, the near-nucleus (small  $r$ ) behavior of the Pauli potential is

$$v_\theta^{(2)}(r) = C_1^{(2)} \frac{(1 + C_2^{(2)} b_1 \alpha)}{b_1 \alpha^2} + O(r), \quad (65)$$

with constants  $C_i^{(2)} > 0$  which depend on the specific density behavior being handled.

The RDDs considered thus far are combinations of powers of  $s$  and  $p$  which ensure cancellation of nuclear cusp divergences in  $v_\theta$ . Thus, we define a class of approximate KE functionals, the reduced derivative approximation (RDA) functionals, as those with enhancement factors depending on the RDDs

$$T_s^{\text{RDA}}[n] \equiv T_W[n] + \int t_0([n]; \mathbf{r}) F_\theta(\kappa_2(\mathbf{r}), \tilde{\kappa}_4(\mathbf{r})) d^3 \mathbf{r}, \quad (66)$$

( $t_0[n]$  from Eq. (5)) with non-divergent Pauli potentials as a consequence of constraints imposed on the coefficients in the RDDs. This route of development of KE functionals is under active investigation; see below.

For insight, Figure 5 shows the behavior of the RDD  $\tilde{\kappa}_4$  along the SiO internuclear axis for four values of  $b_2$ . The behavior in the vicinity of the Si atom is shown. Both the  $s$  and  $p$  variables have four maxima which lie close to the intershell minima in the density. Increasing the value of  $b_2$  increases the height of the corresponding maxima for  $\tilde{\kappa}_4$  RDD (because the contributions from the  $p$ -maxima increase).

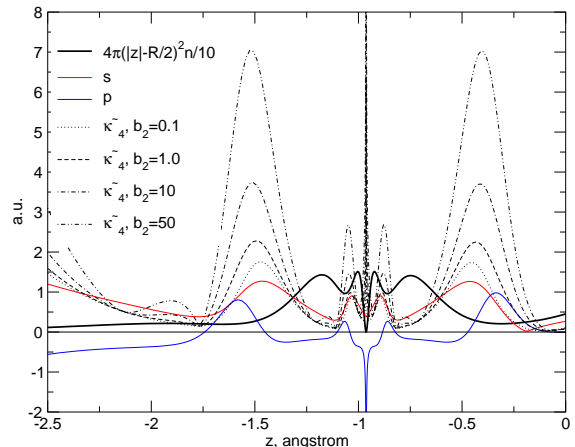


FIG. 5: The fourth order,  $\tilde{\kappa}_4$  reduced density derivative for different values of  $b_2$  along the internuclear axis  $z$  for the SiO diatomic molecule near the Si atom: Si at  $(0, 0, -0.963)\text{\AA}$ , O at  $(0, 0, +0.963)\text{\AA}$ . Variables  $s$  and  $p$ , are shown for comparison.

One of the peculiarities is that the reduced density Laplacian  $p$  is divergent at the nucleus and, as a consequence,  $\tilde{\kappa}_4$  itself also is divergent, even though it generates a non-divergent  $v_\theta$ . This divergence will not affect the KE enhancement factors provided that  $\lim_{\tilde{\kappa}_4 \rightarrow \infty} F_\theta(\tilde{\kappa}_4) = \text{Constant}$ . One of the advantages of the  $\tilde{\kappa}_4$  variable is its positiveness everywhere (by definition).

## B. Parameterization of a RDA functional

In addition to the positive singularities, another limitation of our earlier modified-conjoint type KE functionals was the inability to parameterize them to provide both forces and total energies simultaneously<sup>7</sup>. Given the emphasis on MD simulations, parameterization to the forces was the priority. With the spurious repulsive singularities removed from RDD functionals, the question arises whether total energy parameterization can be used and, if so, if it is beneficial. The usual *energy* fitting criterion is to minimize

$$\omega_E = \sum_{i=1}^m |E_i^{\text{KS}} - E_i^{\text{OF-DFT}}|^2, \quad (67)$$

over systems (e.g., atoms, molecules) and configurations (e.g., diatomic molecule bond length) indexed generically here by  $i$ . When the parameter adjustment is done for fixed-density inputs (i.e., conventional KS densities as inputs), this total energy optimization is equivalent to optimization of the  $T_s$  functional. We did this for determination of the empirical parameters for the new RDA-type functionals  $F_\theta^{\text{RDA}} = F_\theta(\tilde{\kappa}_4)$ .

Since  $F_\theta = 1$  (or any constant in general) also yields a non-singular Pauli potential, we can form  $\tilde{\kappa}_4$ -dependent

enhancement factors which resemble GGA forms and thereby enable connection with the modified conjoint GGA functionals discussed already. One form which we have begun exploring (see below) is

$$F_{\theta}^{\text{RDA}(ij)}(\tilde{\kappa}_4) = A_0 + A_1 \left( \frac{\tilde{\kappa}_4}{1 + \beta_1 \tilde{\kappa}_4} \right)^i + A_2 \left( \frac{\tilde{\kappa}_4}{1 + \beta_2 \tilde{\kappa}_4} \right)^j. \quad (68)$$

$A_i$  and  $\beta_i$  are parameters to be determined. Even this simple form has two desirable properties: (i) the corresponding  $v_{\theta}$  is finite for densities with the near-nucleus behavior defined by Eq. (59), hence also Eqs. (25) or (26) (this has been checked by explicit analytical calculation); (ii) the divergence of  $\tilde{\kappa}_4$  near the nucleus (see Figure 5) cancels in Eq. (68) ( $\lim_{\tilde{\kappa}_4 \rightarrow \infty} F_{\theta}^{\text{RDA}(ij)}(\tilde{\kappa}_4) = A_0 + A_1/\beta_1^i + A_2/\beta_2^j$ ). Positivity of  $F_{\theta}^{\text{RDA}(ij)}$  depends on the parameters  $A_i$  and must be checked for any given determination of their values.

After limited exploration, we used  $i=2$ ,  $j=4$ . Again because the motivating materials problem was brittle fracture in the presence of water, our choice of training sets tended to focus on SiO. We used two molecules with Si-O bonds and two closed shell atoms,  $M = \{\text{H}_6\text{Si}_2\text{O}_7, \text{H}_4\text{SiO}_4, \text{Be}, \text{Ne}\}$ , with a set of six bond lengths for each molecule. That is, for the  $\text{H}_6\text{Si}_2\text{O}_7$  one of the central Si-O bond lengths was changed,  $R(\text{Si}_1\text{-O}_1) = \{1.21, 1.41, 1.61, 1.91, 2.21, 2.81\}$  Å. For  $\text{H}_4\text{SiO}_4$ , the deformation was in  $T_d$  mode: all four Si-O bonds were changed identically,  $R(\text{Si-O}_i) = \{1.237, 1.437, 1.637, 1.937, 2.237, 2.437\}$  Å. KS-LDA densities and energies were the inputs (again see Appendix B for computational details). Minimization of the target function defined by Eq. (67) gave  $b_2=46.56873$ ,  $A_0=0.51775$ ,  $A_1=3.01873$ ,  $\beta_1=1.30030$ ,  $A_2=-0.23118$ , and  $\beta_2=0.59016$ . A simple check shows that the resulting enhancement factor  $F_{\theta}^{\text{RDA}(24)}(\tilde{\kappa}_4)$  is positive for all positive values of  $\tilde{\kappa}_4$  (recall that  $\tilde{\kappa}_4$  is positive by definition). Figures 6 and 7 show the  $F_{\theta}^{\text{RDA}(24)}$  enhancement factor as a function of  $s^2$  for selected values of  $p$  and, reciprocally, as a function of  $p$  for selected values of  $s^2$ . This is a smooth, positive function.  $F_{\theta}^{\text{RDA}(24)}(s^2, p \geq 0.4)$  becomes practically a straight line, essentially independent of  $s^2$ .

Table I displays kinetic energies for 14 molecules (four of them with Si-O bonds) calculated at equilibrium geometries by the conventional KS method and by approximate OF-DFT functionals using the KS density as input. The Thakkar empirical functional<sup>49</sup> was chosen as an example of a GGA KE functional. The Perdew-Constantin meta-GGA<sup>19</sup> ‘‘MGGA’’ was chosen because it, like our functional, is based on quantities that are at fourth order in the density gradient expansion. The results are a bit surprising, because the mean absolute error (MAE) for the RDA functional is almost a factor of two smaller than the MAE for the Thakkar KE, and almost ten times smaller than the MAE for the MGGA. Given the param-

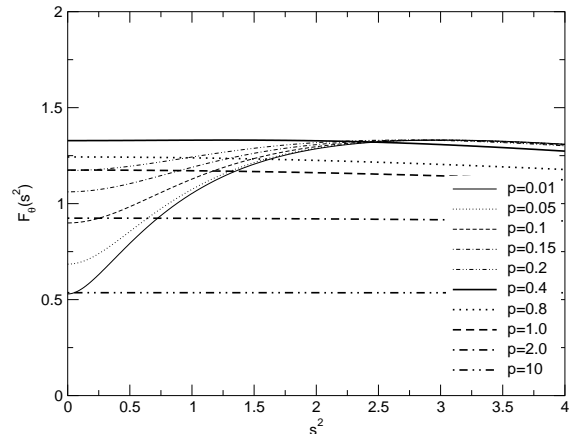


FIG. 6: The RDA(24) enhancement factor as a function of  $s^2$  for selected values of  $p$ .

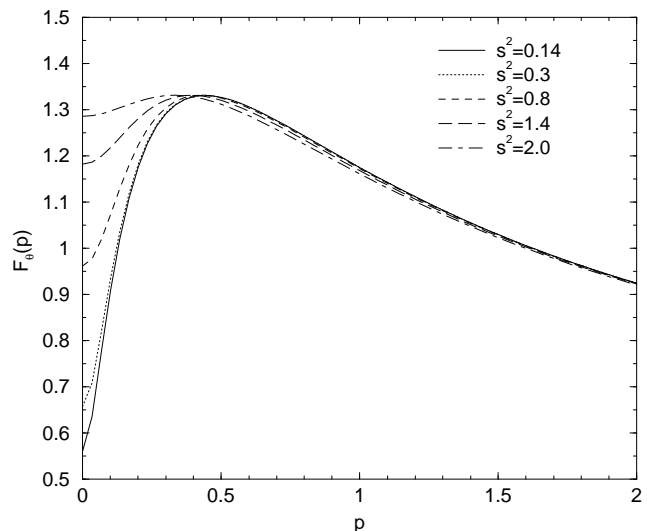


FIG. 7: The RDA(24) enhancement factor as a function of  $p$  for selected values of  $s^2$ .

eterization to a small training set containing only two molecules with Si-O bonds and two closed shell atoms, we had not expected to obtain such good transferability to other systems.

Because our objective is a KE functional capable of predicting correct interatomic forces, one of the important aspects is the behavior in the attractive regions of the potential surface. Table II shows energy gradients for the molecules in Table I calculated at the stretched bond length(s) for which the ‘‘exact’’ (i.e. reference) KS attractive force has maximum magnitude. One and two bonds were deformed in the water molecule (respectively denoted in the table as  $\text{H}_2\text{O}(1\text{R})$  and  $\text{H}_2\text{O}(2\text{R})$ ), while  $\text{SiH}_4$  and  $\text{H}_4\text{SiO}_4$  were deformed in  $T_d$  mode, and only one Si-O bond was stretched in  $\text{H}_4\text{SiO}$  and  $\text{H}_6\text{Si}_2\text{O}_7$ .

The forces were calculated by a three-point centered

TABLE I: KS kinetic energy  $T_s$  values (in Hartrees) for selected molecules and differences ( $T_s^{\text{OF-DFT}} - T_s^{\text{KS}}$ ) calculated using a GGA (Thakkar), MGGA, and RDA(24) explicit semi-local approximate functionals. LDA-KS densities for LDA equilibrium geometries (calculated as described in Appendix B) were used as input.

	KS	Thakkar	MGGA	RDA(24)
H <sub>2</sub>	1.080	-0.022	0.103	0.006
LiH	7.784	0.021	0.296	0.063
H <sub>2</sub> O	75.502	-0.285	0.318	-0.128
HF	99.390	-0.353	0.329	-0.148
N <sub>2</sub>	108.062	-0.340	0.300	-0.041
LiF	106.183	-0.261	0.566	0.086
CO	111.832	-0.333	0.300	-0.074
BF	123.117	-0.273	0.456	0.077
NaF	260.097	-0.348	1.295	0.648
SiH <sub>4</sub>	290.282	0.084	3.112	0.381
SiO	362.441	-0.262	2.825	0.293
H <sub>4</sub> SiO	364.672	-0.163	3.338	0.293
H <sub>4</sub> SiO <sub>4</sub>	587.801	-0.860	4.133	-0.034
H <sub>6</sub> Si <sub>2</sub> O <sub>7</sub>	1100.227	-1.408	7.968	0.086
MAE <sup>a</sup>	—	0.358	1.810	0.168

<sup>a</sup> MAE=mean absolute error

TABLE II: Energy gradient (Hartree/Å) calculated at point  $R_m$  corresponding to the extremum of attractive force as calculated by the KS method. Approximate OF-DFT energy gradients are obtained by replacing  $T_s^{\text{KS}}$  by  $T_s^{\text{OF-DFT}}$ . LDA-KS densities for LDA equilibrium geometries (calculated as described in Appendix B) were used as input.

	$R_m, \text{Å}$	KS	Thakkar	MGGA	RDA(24)
H <sub>2</sub>	1.2671	0.164	0.029	0.112	0.005
LiH	2.455	0.046	0.016	0.037	0.016
H <sub>2</sub> O(1R)	1.3714	0.216	-0.050	-0.073	0.249
H <sub>2</sub> O(2R)	1.3714	0.416	-0.127	-0.163	0.424
HF	1.3334	0.232	-0.071	-0.003	0.180
N <sub>2</sub>	1.3986	0.576	-0.349	-0.819	0.244
LiF	2.0405	0.079	-0.019	-0.032	-0.007
CO	1.4318	0.474	-0.248	-0.659	0.466
BF	1.6687	0.207	-0.037	-0.118	0.204
NaF	2.4284	0.067	-0.007	1.169	-0.008
SiH <sub>4</sub>	1.9974	0.447	0.102	0.189	0.101
SiO	1.9261	0.278	-0.098	-0.281	0.175
H <sub>4</sub> SiO	2.057	0.162	-0.027	-0.086	0.151
H <sub>4</sub> SiO <sub>4</sub>	2.037	0.712	-0.278	-0.714	0.745
H <sub>6</sub> Si <sub>2</sub> O <sub>7</sub>	2.010	0.194	-0.022	-0.173	0.165

finite-difference formula. As found in our previous work and summarized above, the GGA functionals (with the Thakkar functional as the example GGA functional here) are generally incapable of predicting the correct sign (attraction) for the force; the only molecules in Table II for which GGA predicts attraction are H<sub>2</sub>, LiH, and SiH<sub>4</sub>. We find the situation with the MGGA functional to be very similar; the predicted energy gradient has the wrong sign in most cases. In contrast, for all but two of the table

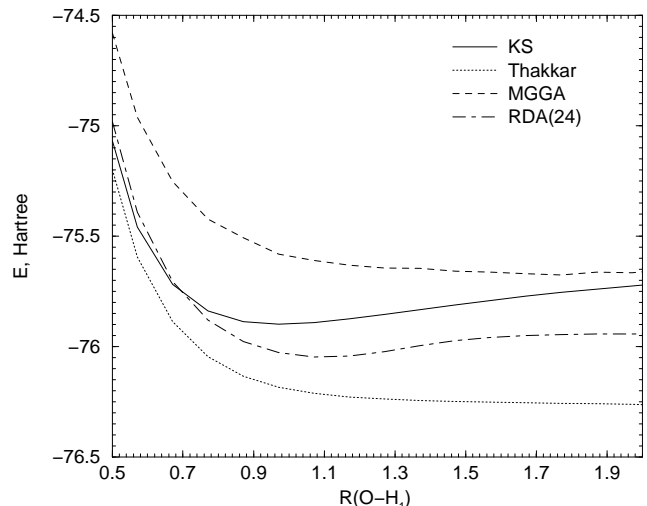


FIG. 8: Total energy as a function of the O-H<sub>1</sub> distance for the H<sub>2</sub>O molecule (with O-H<sub>2</sub> kept at its equilibrium value) obtained from a KS calculation with LDA XC and from approximate GGA(Thakkar), MGGA(Perdew-Constantin) and RDA(24) functionals. The LDA KS densities (calculated as described in Appendix B) were used as input to the orbital-free functionals.

entries the RDA(24) functional predicts the correct sign of the gradient. In many cases (H<sub>2</sub>O(1R), H<sub>2</sub>O(2R), HF, CO, BF, SiO, H<sub>4</sub>SiO, H<sub>4</sub>SiO<sub>4</sub>, H<sub>6</sub>Si<sub>2</sub>O<sub>7</sub>) it yields values very close to the reference KS results.

Figure 8 shows the energy for the water molecule as a function of the O-H<sub>1</sub> bond length. Again, neither the GGA nor the MGGA curve exhibits a minimum. This is a case for which the new RDA(24) functional behaves relatively poorly. It does reproduce a minimum, but at too large a bond length, while in the tail region its curve goes almost flat. Thus the structure predicted by RDA(24) would be more expanded than the correct value and the attractive force in the tail region would be significantly underestimated.

### C. Atomic analysis of the RDA(24) functional

For analysis of the new functional, we calculated the Pauli potential near the nucleus ( $r \rightarrow 0$ ) for the Be atom using a simple H-like density. A single- $\zeta$  Slater orbital density with exponents  $\zeta_{1s} = 3.6848$  and  $\zeta_{2s} = 0.9560$  taken from Ref. 57 near  $r = 0$  has the following Taylor series expansion:  $n(r) \approx 415.0479 \times (1 - 7.3971 r)$ . The density  $n(r) = 415.0479 \times \exp(-7.3971 r)$  has the same slope at  $r = 0$ . It can be used as an approximate density for the Be atom near  $r = 0$  to calculate the Pauli potential for the RDA(24) Eq. (68), for the GGA<sup>44</sup> and for the PBE2 modified conjoint GGA functionals. Calculations were performed using our own MAPLE code. For

RDA(24), we find

$$v_{\theta}^{\text{RDA}(24)}(r \rightarrow 0) = 14010 - 5.9025 \times 10^6 r + 1.1271 \times 10^9 r^2 + O(r^3), \quad (69)$$

while for the GGA the result is

$$v_{\theta}^{\text{GGA}}(r \rightarrow 0) = \frac{-3.1961}{r} + 272.95 - 1319.1 r + 3257.5 r^2 + O(r^3), \quad (70)$$

and for the PBE2 modified conjoint GGA

$$v_{\theta}^{\text{PBE2}}(r \rightarrow 0) = \frac{0.742}{r} + 265.31 - 1319.6 r + 3257.1 r^2 + O(r^3). \quad (71)$$

As expected, the first term in the GGA potential is divergent and negative, while the PBE2 modified conjoint GGA functional has a divergent but positive first term. The numerical coefficients for the rest of the terms are very close for the GGA and PBE2 modified conjoint GGA functionals. This closeness is consistent with the analysis in Ref. 29.

Figure 9 (upper panel) shows the KS-LDA Pauli potential for the Be atom. Its value at the nucleus is approximately 3.5 Hartrees. The RDA(24) potential has a finite (and positive) value at the nucleus, but it is a strong overestimate; recall Eq. (69). Further comparison shows that the slope of the RDA(24) Pauli potential at the nucleus has a large negative value, whereas it should be very close to zero (see upper panel of Fig. 9). To complete the study, three enhancement factors, KS, GGA and RDA(24), are shown in the same panel. Again, as was seen in Figure 3 for the SiO molecule, there is an important region where  $F_{\theta}^{\text{GGA}}$  is negative. The RDA(24) enhancement factor is positive everywhere, but is still far from being an accurate approximation to the KS form.  $F_{\theta}^{\text{RDA}(24)}$  has a sharp minimum near  $r \approx 0.75$  Å which corresponds to the change of sign of the reduced Laplacian of the density ( $p$ ) (see the lower panel). The RDD  $\tilde{\kappa}_4$  (shown in lower panel) also has a sharp minimum near this point.

## V. DISCUSSION AND CONCLUSIONS

Success for the OF-DFT calculation of quantum forces in molecular dynamics requires a reliable explicit form for  $T_s$ . Though previously published GGA-type (conjoint and nearly so) KE functionals yield reasonable KE values, they fail to bind simple molecules even with the correct KS density as input. Therefore they produce completely unusable interatomic forces. This poor performance stems from violation of the positivity requirement on the Pauli potential. Our first remedy was to constrain conjoint KE functionals to yield positive-definite Pauli potentials. Those functionals generate bound molecules and give semi-quantitative inter-atomic forces. However,

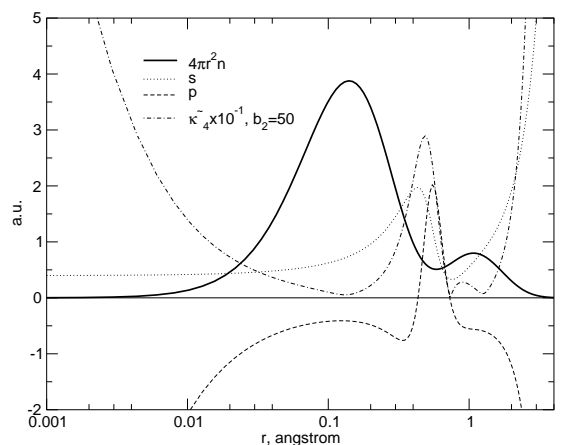
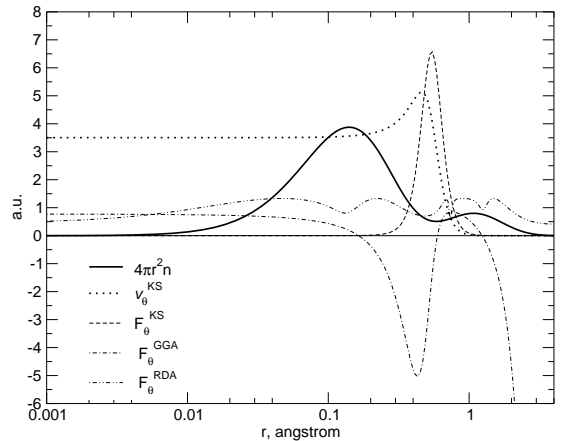


FIG. 9: (Upper panel): numerical KS-LDA density of the Be atom, KS Pauli potential and corresponding enhancement factor, and two approximate enhancement factors. (Lower panel): variables  $s$ ,  $p$ ,  $\tilde{\kappa}_4$  ( $b_2 = 50$ ) calculated for the Be atom using KS-LDA density (also shown).

they are singular at the nuclear positions, hence severely over-estimate the KS kinetic energy. Examination of the near-nucleus behavior of both original conjoint and modified-conjoint GGA functionals shows that the singularities cannot be eliminated within that simple functional form.

Truncation of the gradient expansion, at higher orders in  $s$  and  $p$ , allows us to identify near-nucleus singular behavior and obtain relationships among the coefficients of those truncations that will eliminate such singularities. The resulting reduced density derivatives and related reduced-density-approximation functionals are promising for the simultaneous description of kinetic energies and interatomic forces.

Two other aspects of the numerical results in Table I relate to exact constraints, hence deserve brief comment. First, the von Weizsäcker KE is the exact  $T_s$  for two-

electron singlets. We have not enforced that limit, yet the error from RDA(24) in  $H_2$  is only 6 mHartree. Second, violation of  $N$ -representability by an approximate  $T_s^{\text{appx}}[n]$  is signaled by  $T_s^{\text{appx}}[n] - T_s[n] < 0$  for at least one  $n^{58}$ . Five of the RDA(24) entries in Table I have such negative differences, while MGGA has none and the earlier GGA by Thakkar has many. However, interpretation of those computed differences is a bit tricky, in that they do not correspond to the rigorous  $N$ -representability-violation test but to  $T_s^{\text{appx}}[n] - T_s^{\text{LDA}}[n]$ . With that limitation in mind, the results in Table I are at least suggestive of the notion that the MGGA and RDA(24) functionals are  $N$ -representable or, in some operational sense, close. It is also important to remember that the narrow goal is a functional that can be parameterized to a small training set which is relevant to the desired materials simulations. This limitation of scope is a practical means for limiting the risks of non- $N$ -representability. In addition, we have many RDD forms open for exploration other than RDA(24).

We close with a final word of caution. The functional forms we have examined to this point, e.g. Eq. (68), may be too simple to provide robust and transferable KE functionals for practical OF-DFT applications. Moreover, the use of RDDs as basic variables in kinetic energy enhancement factors guarantees the finiteness of the corresponding Pauli potential only for those densities which satisfy a generalization of Kato's cusp condition Eq. (59), and does not guarantee the satisfaction of the non-negativity property, Eqs. (15)–(16). The latter constraint must be enforced separately. Nevertheless the RDA scheme appears quite promising and further development of it is underway.

### Acknowledgments

We acknowledge informative conversations with Paul Ayers, Mel Levy, Eduardo Ludeña, John Perdew, Yan Alexander Wang, and Tomasz Wesolowski. This work was supported in part by the U.S. National Science Foundation, grant DMR-0325553. FEH also acknowledges support from NSF grant PHY-0601758.

### APPENDIX A. FUNCTIONAL DERIVATIVES OF $F_\theta$

This appendix provides detail relative to derivation of the formulas given in Eqs. (24), (47), and (48). All of them follow from an evaluation of an expression of the generic form presented as  $v_\theta^{(2i)}(\mathbf{r})$ , Eq. (46). That equation is a straightforward expression of the rules for the evaluation of a functional derivative. For clarity in what follows, we restate here the definitions

$$s^2 = \frac{\nabla n \cdot \nabla n}{\xi^2 n^{8/3}}, \quad p = \frac{\nabla^2 n}{\xi^2 n^{5/3}}, \quad t_0([n]; \mathbf{r}) = c_0 n^{5/3}, \quad (72)$$

where  $\xi^2 = 4(3\pi^2)^{2/3}$  and  $c_0 = \frac{3}{10}(3\pi^2)^{2/3}$ . We also remind the reader that

$$q = \frac{\nabla n \cdot \nabla \nabla n \cdot \nabla n}{\xi^4 n^{13/3}}, \quad q' = \frac{\nabla n \cdot \nabla \nabla^2 n}{\xi^4 n^{10/3}},$$

$$q'' = \frac{\nabla^4 n}{\xi^4 n^{7/3}}, \quad q''' = \frac{\nabla \nabla n : \nabla \nabla n}{\xi^4 n^{10/3}}; \quad (73)$$

recall that  $A : B \equiv \sum_{ij} A_{ij} B_{ji}$ . In addition, we introduce the sixth-order reduced density derivatives

$$h = \frac{|\nabla n \cdot \nabla \nabla n|^2}{\xi^6 n^6}, \quad h' = \frac{|\nabla \nabla^2 n|^2}{\xi^6 n^4},$$

$$h'' = \frac{(\nabla \nabla^2 n) \cdot (\nabla \nabla n \cdot \nabla n)}{\xi^6 n^5}. \quad (74)$$

Finally, we write  $n$  instead of the more explicit form  $n(\mathbf{r})$ , and we note that the derivatives of  $s^2$  and  $p$  with respect to  $n$ ,  $\nabla n$ , and  $\nabla^2 n$  are

$$\frac{\partial(s^2)}{\partial n} = -\frac{8s^2}{3n}, \quad \frac{\partial(s^2)}{\partial(\nabla n)} = \frac{2\nabla n}{\xi^2 n^{8/3}}, \quad \frac{\partial(s^2)}{\partial(\nabla^2 n)} = 0;$$

$$\frac{\partial p}{\partial n} = -\frac{5p}{3n}, \quad \frac{\partial p}{\partial(\nabla n)} = 0, \quad \frac{\partial p}{\partial(\nabla^2 n)} = \frac{1}{\xi^2 n^{5/3}}. \quad (75)$$

Substituting these relations into Eq. (46), and restricting consideration to cases where  $F_\theta$  depends only on  $s^2$  and  $p$  (for which all the terms we need to use are explicitly shown in that equation), we have immediately

$$v_\theta(\mathbf{r}) = c_0 n^{2/3} \left[ \frac{5}{3} F_\theta - \frac{8}{3} s^2 \left( \frac{\partial F_\theta}{\partial(s^2)} \right) - \frac{5}{3} p \left( \frac{\partial F_\theta}{\partial p} \right) \right]$$

$$- \frac{2c_0}{\xi^2} \nabla \cdot \left[ \left( \frac{\partial F_\theta}{\partial(s^2)} \right) \frac{\nabla n}{n} \right] + \frac{c_0}{\xi^2} \nabla^2 \left( \frac{\partial F_\theta}{\partial p} \right). \quad (76)$$

At this point we remark that some terms that would otherwise be expected in Eq. (46) are absent because of the zeros in Eq. (75).

To proceed further we need to expand the last two terms of Eq. (76). The first of these terms expands into

$$-2c_0 n^{2/3} \left[ \left( \frac{\partial F_\theta}{\partial(s^2)} \right) \left\{ \frac{\nabla(n^{-1}) \cdot \nabla n + n^{-1} \nabla^2 n}{\xi^2 n^{2/3}} \right\} \right.$$

$$\left. + \left( \frac{\partial^2 F_\theta}{\partial(s^2)^2} \right) \frac{\nabla s^2 \cdot \nabla n}{\xi^2 n^{5/3}} + \left( \frac{\partial^2 F_\theta}{\partial p \partial(s^2)} \right) \frac{\nabla p \cdot \nabla n}{\xi^2 n^{5/3}} \right]. \quad (77)$$

Observing now that  $\nabla(n^{-1}) = -n^{-2} \nabla n$  and that

$$\nabla(s^2) = -\frac{8s^2}{3n} \nabla n + \frac{2\nabla n \cdot \nabla \nabla n}{\xi^2 n^{8/3}},$$

$$\nabla p = \frac{\nabla \nabla^2 n}{\xi^2 n^{5/3}} - \frac{5}{3} \frac{(\nabla^2 n) \nabla n}{\xi^2 n^{8/3}}, \quad (78)$$

the expression in Eq. (77) can be brought to the form

$$\begin{aligned}
& +2c_0 n^{2/3} \left[ (s^2 - p) \left( \frac{\partial F_\theta}{\partial (s^2)} \right) \right. \\
& + \left( \frac{8}{3} s^4 - 2q \right) \left( \frac{\partial^2 F_\theta}{\partial (s^2)^2} \right) \\
& \left. - \left( q' - \frac{5}{3} s^2 p \right) \left( \frac{\partial^2 F_\theta}{\partial p \partial (s^2)} \right) \right]. \quad (79)
\end{aligned}$$

Continuing now to the final term of Eq. (76), we ex-

pand the Laplacian, obtaining initially

$$\begin{aligned}
\frac{c_0}{\xi^2} \nabla^2 \left( \frac{\partial F_\theta}{\partial p} \right) &= c_0 n^{2/3} \left[ \left( \frac{\partial^2 F_\theta}{\partial (s^2) \partial p} \right) \frac{\nabla^2 s^2}{\xi^2 n^{2/3}} \right. \\
& + \left( \frac{\partial^2 F_\theta}{\partial p^2} \right) \frac{\nabla^2 p}{\xi^2 n^{2/3}} + \left( \frac{\partial^3 F_\theta}{\partial (s^2)^2 \partial p} \right) \frac{\nabla s^2 \cdot \nabla s^2}{\xi^2 n^{2/3}} \\
& \left. + 2 \left( \frac{\partial^3 F_\theta}{\partial (s^2) \partial p^2} \right) \frac{\nabla s^2 \cdot \nabla p}{\xi^2 n^{2/3}} + \left( \frac{\partial^3 F_\theta}{\partial p^3} \right) \frac{\nabla p \cdot \nabla p}{\xi^2 n^{2/3}} \right]. \quad (80)
\end{aligned}$$

Using Eqs. (78), we next find

---


$$\begin{aligned}
\nabla^2 s^2 &= -\frac{8}{3} \nabla \cdot \left( \frac{s^2}{n} \nabla n \right) + \frac{2}{\xi^2} \nabla \cdot \left( \frac{\nabla n \cdot \nabla \nabla n}{n^{8/3}} \right) \\
&= -\frac{8}{3} \left[ -\frac{s^2}{n^2} \nabla n \cdot \nabla n + \frac{\nabla (s^2) \cdot \nabla n}{n} + \frac{s^2}{n} \nabla^2 n \right] + \frac{2}{\xi^2} \left[ -\frac{8}{3} \frac{\nabla n \cdot \nabla \nabla n \cdot \nabla n}{n^{11/3}} + \frac{\nabla \nabla n : \nabla \nabla n + \nabla n \cdot \nabla \nabla^2 n}{n^{8/3}} \right], \\
\nabla^2 p &= \frac{1}{\xi^2} \nabla \cdot \left( \frac{\nabla \nabla^2 n}{n^{5/3}} \right) - \frac{5}{3\xi^2} \nabla \cdot \left( \frac{(\nabla^2 n) \nabla n}{n^{8/3}} \right) \\
&= \frac{1}{\xi^2} \left[ -\frac{5}{3} \frac{\nabla \nabla^2 n \cdot \nabla n}{n^{8/3}} + \frac{\nabla^4 n}{n^{5/3}} \right] - \frac{5}{3\xi^2} \left[ -\frac{8}{3} \frac{(\nabla^2 n) \nabla n \cdot \nabla n}{n^{11/3}} + \frac{(\nabla^2 n)^2}{n^{8/3}} + \frac{\nabla \nabla^2 n \cdot \nabla n}{n^{8/3}} \right], \\
\nabla s^2 \cdot \nabla s^2 &= \frac{64s^4}{9n^2} \nabla n \cdot \nabla n - \frac{32s^2}{3} \frac{\nabla n \cdot \nabla \nabla n \cdot \nabla n}{\xi^2 n^{11/3}} + 4 \frac{|\nabla n \cdot \nabla \nabla n|^2}{\xi^4 n^{16/3}}, \\
\nabla s^2 \cdot \nabla p &= -\frac{8s^2}{3} \frac{\nabla n \cdot \nabla \nabla^2 n}{\xi^2 n^{8/3}} + 2 \frac{(\nabla \nabla^2 n) \cdot (\nabla n \cdot \nabla \nabla n)}{\xi^4 n^{13/3}} + \frac{40s^2}{9} \frac{(\nabla^2 n) \nabla n \cdot \nabla n}{\xi^2 n^{11/3}} - \frac{10}{3} \frac{(\nabla^2 n) \nabla n \cdot \nabla \nabla n \cdot \nabla n}{\xi^4 n^{16/3}}, \\
\nabla p \cdot \nabla p &= \frac{|\nabla \nabla^2 n|^2}{\xi^4 n^{10/3}} - \frac{10}{3} \frac{(\nabla^2 n) \nabla \nabla^2 n \cdot \nabla n}{\xi^4 n^{13/3}} + \frac{25}{9} \frac{(\nabla^2 n)^2 \nabla n \cdot \nabla n}{\xi^4 n^{16/3}}. \quad (81)
\end{aligned}$$

Then, combining material from Eqs. (76), (79), (80), and (81), and introducing the notations in Eqs. (72)–(74), we obtain the final result, applicable for any  $F_\theta$  that depends only on  $s$  and  $p$ :

$$\begin{aligned}
v_\theta &= c_0 n^{2/3} \left[ \frac{5}{3} F_\theta - \left( \frac{2}{3} s^2 + 2p \right) \left( \frac{\partial F_\theta}{\partial (s^2)} \right) - \frac{5}{3} p \left( \frac{\partial F_\theta}{\partial p} \right) + \left( \frac{16}{3} s^4 - 4q \right) \left( \frac{\partial^2 F_\theta}{\partial (s^2)^2} \right) \right. \\
& + \left( \frac{88}{9} s^4 + \frac{2}{3} s^2 p - \frac{32}{3} q + 2q''' \right) \left( \frac{\partial^2 F_\theta}{\partial (s^2) \partial p} \right) + \left( \frac{40}{9} s^2 p - \frac{5}{3} p^2 - \frac{10}{3} q' + q'' \right) \left( \frac{\partial^2 F_\theta}{\partial p^2} \right) \\
& + \left( \frac{64}{9} s^6 - \frac{32}{3} s^2 q + 4h \right) \left( \frac{\partial^3 F_\theta}{\partial (s^2)^2 \partial p} \right) + \left( \frac{80}{9} s^4 p - \frac{16}{3} s^2 q' - \frac{20}{3} p q + 4h'' \right) \left( \frac{\partial^3 F_\theta}{\partial (s^2) \partial p^2} \right) \\
& \left. + \left( \frac{25}{9} s^2 p^2 - \frac{10}{3} p q' + h' \right) \left( \frac{\partial^3 F_\theta}{\partial p^3} \right) \right]. \quad (82)
\end{aligned}$$

We may now specialize Eq. (82) to the cases needed in the present work. Taking first  $F_\theta^{\text{GGA}}$ , which has no  $p$

dependence, all the terms of Eq. (82) containing derivatives with respect to  $p$  vanish, leaving only the expression

previously given as Eq. (24).

Turning next to the specific forms of  $F_\theta$  discussed in Section IV-A, we note that  $F_\theta^{\text{SGA}} = 1 + a_2 s^2$  is not only independent of  $p$ , but is also linear in  $s^2$ , so  $\partial F_\theta / \partial (s^2) = a_2$  and  $\partial^2 F_\theta / \partial (s^2)^2 = 0$ . This causes  $v_\theta^{\text{SGA}}$  to have the form

$$v_\theta^{\text{SGA}} = c_0 n^{2/3} \left[ \frac{5}{3} (1 + a_2 s^2) - a_2 \left( \frac{2}{3} s^2 + 2p \right) \right], \quad (83)$$

which simplifies to the result given in Eq. (47).

Finally, we consider  $F_\theta^{(4)}$  as given in Eq. (45). All the third derivatives of  $F_\theta$  in Eq. (82) vanish; the first and second derivatives of  $F_\theta$  have simple forms. We have

$$\begin{aligned} v_\theta^{(4)} = & c_0 n^{2/3} \left[ \frac{5}{3} (a_4 s^4 + b_2 p^2 + c_{21} s^2 p) \right. \\ & - \left. \left( \frac{2}{3} s^2 + 2p \right) (2a_4 s^2 + c_{21} p) \right. \\ & - \frac{5}{3} p (2b_2 p + c_{21} s^2) + 2a_4 \left( \frac{16}{3} s^4 - 4q \right) \\ & + c_{21} \left( \frac{88}{9} s^4 + \frac{2}{3} s^2 p - \frac{32}{3} q + 2q''' \right) \\ & \left. + 2b_2 \left( \frac{40}{9} s^2 p - \frac{5}{3} p^2 - \frac{10}{3} q' + q'' \right) \right]. \quad (84) \end{aligned}$$

Equation (84) simplifies to the result given as Eq. (48).

## APPENDIX B. COMPUTATIONAL METHODS

We assess functionals by comparing results from them with those of conventional orbital-dependent Kohn-Sham calculations in the local density approximation (LDA), using standard methods described in, for example, Refs. 59,60,61,62,63,64,65,66. The reference molecular KS calculations were done with a triple-zeta basis with polarization functions (TZVP)<sup>67,68,69</sup>. All integrals were calculated by a numerical integration scheme that, following Becke<sup>70</sup>, uses weight functions localized near each center to represent the multicenter integrals exactly as a sum of (distorted) atomic integrals. Radial integration of the resulting single-center forms is accomplished by a Gauss-Legendre procedure, while integration over the angular variables is done with high-order quadrature formulas developed by Lebedev and coworkers<sup>71,72</sup> with routines downloaded from Ref. 73. These computations were performed using routines developed by Salvador and Mayer<sup>74</sup> and included in their code FUZZY. The Vosko-Wilk-Nussair LDA<sup>65</sup> was used.

Given the KS density, for each OF functional under study we computed the total energy  $E^{\text{OF-DFT}}$  from Eq. (2) and the interatomic forces from Eq. (4). The result is a non-self-consistent calculation which tests whether a given OF functional can reproduce  $T_s[n_{KS}]$ , or at least  $\nabla_{\mathbf{R}} T_s[n_{KS}]$  if  $n_{KS}$  is provided. There is no sense in trying to solve Eq. (3) with an approximate OF functional that cannot pass this test.

---

\* Electronic address: vkarasev@qtp.ufl.edu

† Electronic address: trickey@qtp.ufl.edu

<sup>1</sup> For detailed information and publication references on Car-Parrinello Molecular Dynamics (CPMD), see URL [www.cpmid.org/cpmid.html](http://www.cpmid.org/cpmid.html).

<sup>2</sup> D.E. Taylor, V.V. Karasiev, K. Runge, S.B. Trickey, and F.E. Harris, *Comp. Mater. Sci.* **39**, 705 (2007).

<sup>3</sup> F.H. Streitz and J.W. Mintmire, *Phys. Rev. B* **50**, 11996 (1994).

<sup>4</sup> M.J. Buehler, A.C. van Duin, and W.A. Goddard III, *Phys. Rev. Lett.* **96**, 095505 (2006).

<sup>5</sup> A.K. Rappe and W.A. Goddard III, *J. Phys. Chem.* **95**, 3358 (1991).

<sup>6</sup> V.V. Karasiev, S.B. Trickey, and F.E. Harris, *Chem. Phys.* **330**, 216 (2006).

<sup>7</sup> V.V. Karasiev, S.B. Trickey, and F.E. Harris, *J. Comp.-Aided Mater. Des.* **13**, 111 (2006).

<sup>8</sup> "Recent advances in developing orbital-free kinetic energy functionals", V.V. Karasiev, R.S. Jones, S.B. Trickey, and F.E. Harris, in *New Developments in Quantum Chemistry*, J.L. Paz and A.J. Hernández eds. (Research Signposts), in press.

<sup>9</sup> P. Hohenberg and W. Kohn, *Phys. Rev. B* **136**, 864 (1964).

<sup>10</sup> R.G. Parr and W. Yang, *Density Functional Theory of Atoms and Molecules* (Oxford, New York, 1989).

<sup>11</sup> R.M. Dreizler and E.K.U. Gross, *Density Functional Theory* (Springer-Verlag, Berlin, 1990).

<sup>12</sup> L.H. Thomas, *Proc. Cambridge Phil. Soc.* **23**, 542 (1927).

<sup>13</sup> E. Fermi, *Atti Accad. Nazl. Lincei* **6**, 602 (1927).

<sup>14</sup> C.F. von Weizsäcker, *Z. Phys.* **96**, 431 (1935).

<sup>15</sup> E.V. Ludeña and V.V. Karasiev, in *Reviews of Modern Quantum Chemistry: a Celebration of the Contributions of Robert Parr*, edited by K.D. Sen (World Scientific, Singapore, 2002) pp. 612–665.

<sup>16</sup> Y. A. Wang and E. A. Carter, "Orbital-free Kinetic-energy Density Functional Theory", Chap. 5 in *Theoretical Methods in Condensed Phase Chemistry*, edited by S. D. Schwartz (Kluwer, NY, 2000) pp. 117–184.

<sup>17</sup> B.-J. Zhou and Y.A. Wang, *J. Chem. Phys.* **124**, 081107 (2006).

<sup>18</sup> D. García-Aldea and J.E. Alvarellos, *Phys. Rev. A* **77**, 022502 (2008); *J. Chem. Phys.* **127**, 144109 (2007) and references in both.

<sup>19</sup> J. P. Perdew and L.A. Constantin, *Phys. Rev. B* **75**, 155109 (2007).

<sup>20</sup> C.J. Garcia-Cervera, *Commun. Computat. Phys.* **3**, 968 (2008).

<sup>21</sup> L.M. Ghiringhelli and L. Delle Site, *Phys. Rev. B* **77**, 073104 (2008)

<sup>22</sup> W. Eek and S. Nordholm, *Theoret. Chem. Accounts* **115**,

- 266 (2006).
- <sup>23</sup> W. Kohn and L.J. Sham, Phys. Rev. **140**, A1133 (1965).
- <sup>24</sup> E. Teller, Rev. Mod. Phys. **34**, 627 (1962).
- <sup>25</sup> Y. Tal and R.F.W. Bader, Int. J. Quantum Chem. **S12**, 153 (1978).
- <sup>26</sup> L.J. Bartolotti and P.K. Acharya, J. Chem. Phys. **77**, 4576 (1982).
- <sup>27</sup> J.E. Harriman, in *Density Matrices and Density Functionals*, R. Erdahl and V.H. Smith Jr. eds. (D. Reidel, Dordrecht, 1987), 359-373.
- <sup>28</sup> M. Levy, and H. Ou-Yang, Phys. Rev. A **38**, 625 (1988).
- <sup>29</sup> J.P. Perdew, Phys. Lett. A **165**, 79 (1992).
- <sup>30</sup> H. Lee, C. Lee, and R.G. Parr, Phys. Rev. A **44**, 768 (1991).
- <sup>31</sup> L.J. Sham, Phys. Rev. A **1**, 969 (1970)
- <sup>32</sup> M. Levy, J.P. Perdew, and V. Sahni, Phys. Rev. A **30**, 2745 (1984).
- <sup>33</sup> C. Herring, Phys. Rev. A **34**, 2614 (1986).
- <sup>34</sup> C.H. Hodges, Can. J. Phys. **51**, 1428 (1973).
- <sup>35</sup> I.M. Gelfand and S.V. Fomin, *Calculus of Variations* (Prentice-Hall, Englewood Cliffs NJ, 1963), p. 42.
- <sup>36</sup> G.A. Korn and T.M. Korn, *Mathematical Handbook for Scientists and Engineers* (McGraw-Hill, NY, 1961).
- <sup>37</sup> T. Kato, Commun. Pure Appl. Math. **10**, 151 (1957).
- <sup>38</sup> W.A. Bingel, Z. Naturforschung A **18**, 1249 (1963).
- <sup>39</sup> R.T. Pack and W.B. Brown, J. Chem. Phys. **45**, 556 (1966)
- <sup>40</sup> N.H. March, I.A. Howard, A. Holas, P. Senet, and V.E. Van Doren, Phys. Rev. A **63**, 012520 (2000).
- <sup>41</sup> E.S. Kryachko and E.V. Ludeña, *Energy Density Functional Theory of Many-Electron Systems* (Kluwer, Dordrecht, 1990).
- <sup>42</sup> The nuclear-electron interaction for the point-nucleus model  $v_{ne}^I(\mathbf{r}) = Z_I/|\mathbf{r} - \mathbf{R}_I|$  is the leading term in  $v_{KS}$  Eq. (3) in the limit  $\mathbf{r} \rightarrow \mathbf{R}_I$ . All other terms in  $v_{KS}$  are finite at nucleus  $I$  and hence are negligible in comparison to  $v_{ne}^I$ . Hence, the solution of Eq. (3) in the vicinity of  $\mathbf{r} = \mathbf{R}_I$  is a hydrogen-like density. Equation(26) is appropriate also for molecular systems; see Ref. 39.
- <sup>43</sup> Zs. Jánosfalvi, K.D. Sen, and Á. Nagy, Phys. Lett. A **344**, 1 (2005).
- <sup>44</sup> F. Tran and T.A. Wesolowski, Int. J. Quantum Chem. **89**, 441 (2002).
- <sup>45</sup> J. P. Perdew, K. Burke, and M. Ernzerhof, Phys. Rev. Lett. **77**, 3865 (1996).
- <sup>46</sup> C. Adamo and V. Barone, J. Chem. Phys. **116**, 5933 (2002).
- <sup>47</sup> D.J. Lacks and R.G. Gordon, J. Chem. Phys. **100**, 4446 (1994).
- <sup>48</sup> A.E. DePristo and J.D. Kress, Phys. Rev. A **35**, 438 (1987).
- <sup>49</sup> A.J. Thakkar, Phys. Rev. A **46**, 6920 (1992).
- <sup>50</sup> R.A. King and N.C. Handy, Phys. Chem. Chem. Phys. **2**, 5049 (2000); Mol. Phys. **99**, 1005 (2001).
- <sup>51</sup> Private communication, L.J. Bartolotti to SBT
- <sup>52</sup> D.R. Murphy, Phys. Rev. A **24**, 1682 (1981).
- <sup>53</sup> W. Yang, Phys. Rev. A **34**, 4575 (1986).
- <sup>54</sup> W. Yang, R.G. Parr, and C. Lee, Phys. Rev. A **34**, 4586 (1986).
- <sup>55</sup> P.W. Ayers, R.G. Parr, and A. Nagy, Int. J. Quantum Chem. **90**, 309 (2001).
- <sup>56</sup> R.G. Parr and S.K. Ghosh, Proc. Natl. Acad. Sci. USA **83**, 3577 (1986).
- <sup>57</sup> E. Clementi and D.L. Raimondi, J. Chem. Phys. **38**, 2686 (1963).
- <sup>58</sup> P.W. Ayers and S. Liu, Phys. Rev. A **75**, 022514 (2007).
- <sup>59</sup> J.C. Slater, Phys. Rev. **81**, 385 (1951).
- <sup>60</sup> J.C. Slater, Phys. Rev. **82**, 538 (1951).
- <sup>61</sup> J.C. Slater, J. Chem. Phys. **43**, S228 (1965).
- <sup>62</sup> R. Gáspár, Acta Phys. Hung. **3**, 263 (1954).
- <sup>63</sup> W. Kohn and L.J. Sham, Phys. Rev. **140**, A1133 (1965).
- <sup>64</sup> B.Y. Tong and L.J. Sham, Phys. Rev. **144**, 1 (1966).
- <sup>65</sup> S.H. Vosko, L. Wilk, and M. Nusair, Can. J. Phys. **58**, 1200 (1980).
- <sup>66</sup> D.M. Ceperley and B.J. Alder, Phys. Rev. Lett. **45**, 566 (1980).
- <sup>67</sup> A. Schäfer, H. Horn, and R. Ahlrichs, J. Chem. Phys. **97**, 2571 (1992)
- <sup>68</sup> A. Schäfer, C. Huber, and R. Ahlrichs, J. Chem. Phys. **100**, 5829 (1994).
- <sup>69</sup> From the Extensible Computational Chemistry Environment Basis Set Database, Version 02/25/04, Molecular Science Computing Facility, Environmental and Molecular Sciences Laboratory, Pacific Northwest Laboratory, P.O. Box 999, Richland, Washington 99352, USA, funded by the U.S. Department of Energy (contract DE-AC06-76RLO). See <http://www.emsl.pnl.gov/forms/basisform.html>
- <sup>70</sup> A.D. Becke, J. Chem. Phys. **88**, 2547 (1988).
- <sup>71</sup> V.I. Lebedev and D.N. Laikov, Dokl. Akad. Nauk **366**, 741 (1999).
- <sup>72</sup> V.I. Lebedev and D.N. Laikov, Dokl. Math. **59**, 477 (1999).
- <sup>73</sup> Computational Chemistry List (CCL) Archives: <http://www.ccl.net/>
- <sup>74</sup> P. Salvador and I. Mayer, J. Chem. Phys. **120**, 5046 (2004).



